# Highlights

- Alkenone analysis on sediment core from Sermilik Fjord, SE Greenland.
- Reconstruction of ocean surface temperature changes of the past 100 years.
- Alkenones advected and represent temperature changes on nearby shelf.
- Warm ocean c. 1940 concurs with increased calving from Helheim Glacier
- Similar to observation from Disko Bay and Jakobshavn Isbræ in West Greenland.

# A 100-year long record of alkenone-derived SST changes by Southeast Greenland

Camilla S. Andresen[1*], Marie-Alexandrine Sicre[2], Fiammetta Straneo[3], David A. Sutherland[4], Torben Schmith[5] Mads Hvid Ribergaard[5], Antoon Kuijpers[1], Jerry M. Lloyd[6]

*[1]Geological Survey of Denmark and Greenland, Department of Marine Geology and Glaciology, Øster Voldgade 10, 1350 Copenhagen K, Denmark, csa@geus.dk*

*[2]Laboratoire des Sciences du Climat et de L'Environnement, Domaine du CNRS, Ave de la Terrasse, 91198 Gif-sur-Yvette, Cedex, France*

*[3]Woods Hole Oceanographic Institution, Department of Physical Oceanography, Woods Hole, MA 02543, USA*

*[4]Department of Geological Sciences, University of Oregon, Eugene, Oregon, USA*

*[5]Danish Meterological Institute, Centre for Ocean and Ice, Lyngbyvej 100, 2100 Copenhagen Ø, Denmark*

*[6]Geography Department, University of Durham, South Road, Durham DH1 3LE, UK*

**corresponding author*

## Abstract

Sediment core ER07 from Sermilik Fjord by Helheim Glacier in Southeast Greenland was analysed for alkenones to document sea surface temperature (SST) changes over the past 100 years. The alkenone SST values, ranging from 8 to 12°C, contrasts with colder values (0-4°C) obtained from recent hydrographic surveys inside the fjord. We suggest that advection of allochtonous alkenones produced in the warm Irminger Current waters circulating on the shelf likely accounts for this difference. The temperature range of the alkenone-derived record is similar to in situ observations of 8-11°C on the shelf just outside Sermilik Fjord, and its variability over the past 100 years resembles the constructed variability over the shelf using remote instrumental data. This suggests that oceanographic changes on the adjacent shelf are linked to regional changes of the Irminger Current and the East Greenland Current. The subsurface water heat content has previously been suggested as an important control on Greenland outlet glacier stability and underlined by an episode

of warm subsurface waters ~ 1940 concurrent with markedly increased calving and retreat of Helheim Glacier. Our results therefore suggest that alkenone-derived SST time series from high-sedimentation rate glacial fjords may provide a new approach for reconstruction of past changes of shelf water properties and variability around Greenland.

**Key words:** Southeast Greenland, Sermilik Fjord, Helheim Glacier, alkenones, sea surface temperature, ocean-cryosphere interaction, outlet glacier stability

## 1. Introduction

In the early part of this century, the Greenland Ice Sheet (GIS) experienced a marked increase in net mass loss (Rignot and Kanagaratnam, 2006; van den Broeke et al., 2009), stimulating research for better understanding how such future glacier changes will affect global sea level rise. In Southeast Greenland, outlet glaciers thinned, accelerated and retreated between 2003 and 2005 (Howat et al., 2007, 2008; Moon and Joughin, 2008; Stearns and Hamilton, 2007; Luckman et al., 2006, Rignot and Kanagaratnam, 2006), and it was suggested that concurrent rising temperatures of subsurface ocean currents may have triggered the onset of this acceleration (Nick et al., 2009; Straneo et al., 2010; 2011, 2012; Murray et al., 2010). Likewise, the early 2000's thinning, retreating and doubling of flow velocity of the Jakobshavn Isbræ in West Greenland has been linked to a pulse of warm waters in the West Greenland Current (WGC) propagating up the West Greenland coast and entering Disko Bay in 1997 (Holland et al., 2008). The exact processes involved in ocean-forced destabilisation of outlet glaciers is still not well understood, but it is believed that rapid submarine melting of calving faces is an important mechanism for glacier calving (Rignot et al., 2002, 2010) and that changes in North Atlantic ocean heat transport may decrease the support from the buttressing ice mélange in front of the glacier margin (Vieli and Nick, 2011).

Ice sheet mass changes of the GIS have only been estimated for the past 20-30 years using satellite data. Likewise, the observational SST record on the continental shelf around Greenland is sparse in space and time, and hydrographic surveys in the near-shore and fjord waters virtually absent prior to 2008 (cf. Straneo et al., 2010; Murray et al., 2010). Therefore, in order to establish a more firm causal relationship between ocean variability and glacier dynamical changes we need to explore longer timescales, which requires the use of proxy records (Andresen et al., 2011, 2012).

In this paper, we present a 100-year long SST time-series based on the $C_{37}$ alkenone from a sediment core retrieved in Sermilik Fjord. Alkenone biomarkers in the open ocean waters are mainly produced by the prymnesiophytae, *Emiliania huxleyi*, growing in the photic zone (Volkman et al., 2000). The unsaturation index of the $C_{37}$ alkenones ($U_{37}^{K'}$) in marine waters has been shown to be highly correlated to water temperature on a global scale (Prahl et al., 1988; Conte et al., 2006). We argue that alkenone SSTs derived from the fjord core are indicative largely of property changes of surface waters occurring just outside of Sermilik Fjord. This conclusion is supported by comparing our results to oceanographic data obtained from the broader shelf region. Finally, we discuss the link between ocean variability and glacier dynamical changes on longer timescales by comparing alkenone SSTs with a proxy record of Helheim Glacier calving.

## 2. Setting

Sermilik Fjord is c. 80 km long with a width varying between 7 and 13 km. The bathymetry documents a U-shaped fjord with steep side walls and depths of 920 m at the mouth and 600 m at the northern end of the fjord extending approximately in a north-south direction (Schjøth et al., 2012). The northern end of the fjord branches into three fjords each containing ice-calving glaciers. The westernmost glacier – the Helheim Glacier – is a fast flowing glacier and the third most prolific exporter of icebergs in Greenland (Rignot and Kanagaratnam, 2006). The two northern glaciers, Midgaard and Fenris Glaciers are far less ice productive compared to Helheim (Mernild et al., 2010).

According to MODIS satellite images for the past few years (http://ocean.dmi.dk/arctic/modis.php), open water conditions occur frequently in the fjord throughout the winter as fjord-ice is broken, likely due to strong currents and storms. A marked ice-mélange, with inter-annually varying extension, is situated in front of the Helheim Glacier.

The oceanographic conditions on the Southeast Greenland shelf are characterized by the East Greenland Current (EGC), which transports cold and fresh sea ice-laden surface waters derived from the Arctic Ocean and glacial melt water from East Greenland that has an inner near coastal branch, the East Greenland Coastal Current (EGCC) (Sutherland and Pickart, 2008) (Fig. 1). Off Southeast Greenland, this cold upper (< 250 m) layer is underlain by warmer and saltier waters derived from the Irminger Current (IC) (Malmberg 1985, Murray et al., 2010), which is a branch of the North Atlantic Current. Deep troughs (300-800 m) transect the shallow shelf (100-200 m) and thereby allow not only the upper cold waters, but also the warm subsurface waters to circulate within the Sermilik Fjord, either through estuarine circulation (Murray et al., 2010) or shelf-driven exchange (Straneo et al., 2010). Hence, the hydrographic conditions in Sermilik Fjord are characterized by a two-layer stratification with warm (3.5 to 4°C) IC-derived waters from a depth of 200-300 m and downwards overlain by -1 to +1°C cold Polar Waters advected by the EGC-EGCC water mass system (Fig. 2). In summer, the uppermost 10-20 m are characterised by low-salinity waters from glacier runoff and the temperature can be up to several °C due to solar heating (Straneo et al., 2010).

Interaction between the IC and EGC/EGCC over the shelf influences temperatures and the interface depth (i.e. the thermocline), potentially altering the amount of heat reaching the glacier margins and its ice-mélange in the fjord (Straneo et al., 2010, 2011; Sutherland et al., 2013).

## 3. Methods

Alkenone analysis was carried out on sediment core ER07 obtained from Sermilik fjord (Fig. 1B). This core was retrieved from 525 m water depth (66°00'59"N, 37°51'07"W) and dated by means of $^{210}Pb$ chronology and analysed for grain size composition using a Malvern laser sedigraph. The chronology was calculated using the CRS-model (Constant Rate of Supply (Appleby and Oldfield, 1978) and calculations of the activities of unsupported $^{210}Pb$ in the lower part of the cores were based on regression of activity versus accumulated mass depth in order to increase the robustness of the age models. Further details on methodologies behind ER07 $^{210}Pb$ chronology and sedimentology are provided in Andresen et al. (2012). The upper 24 cm of ER07 was sampled continuously every ½ cm for alkenone determination leading to 43 levels to be analysed (higher sampling density in the upper part of the core).

Alkenones were extracted from freeze-dried sediments using a dichloromethane/methanol mixture (2:1 v/v) and isolated from the total lipid extract by silicagel chromatography (Ternois et al., 1999). The purified fractions were then analysed by gas chromatography using a Varian 3400CX gas chromatograph and a CPSil5 capillary column (50m length, 0.3 2i.d., 0.25 µm film thickness) equipped with a FID detector and a septum programmable injector (SPI). Helium was used as a carrier gas. The $C_{37}$ alkenone distribution comprises $C_{37:3,}$ $C_{37:2}$ and $C_{37:4}$ as expected from cold and low salinity waters of the Northern Hemisphere. While $C_{37:4}$ notably is absent in Southern ocean polar waters (Ternois et al., 1998), its presence in high abundances has been reported in the Nordic Seas (Sicre et al., 2002 ; Bendle et al., 2005), the Baltic

Sea (Shulz et al., 2011) and more recently in Greenland lakes (D'Andrea et al., 2011) suggesting a production that might be linked to species other than E. *huxleyi*.

However, the compilation of open-ocean water samples of Sikes and Sicre (2002) showed that at cold temperatures, even when $C_{37:4}$ is abundant, the use of $U_{37}^{K}$ $(C_{37:2} - C_{37:4})/(C_{37:2} + C_{37:3} + C_{37:4})$ instead of $U_{37}^{K'}$ $(C_{37:2})/(C_{37:2} + C_{37:3})$ does not improve SST estimates and we therefore use the $U_{37}^{K'}$index to calculate temperatures. In coastal regions such as estuarine or fjords, where other species presumably contribute to alkenone production and where $C_{37:4}$ is abundant even at elevated T, local calibration are needed for both indexes.

## 4. Results

Core ER07 is massive diamiction facies and contains on average 20 % sand in the 63-1000 µm fraction, 45 % silt and 35 % clay (Fig. 3A). The upper 24 cm represent the last 100 years according to $^{210}Pb$ chronology (Fig. 3B-C). The time resolution is on average 2.5 years per sample and age uncertainties are in the order of +/- 2-6 years.

The $C_{37}$ alkenone distribution is dominated by $C_{37:4}$ in Sermilik Fjord sediments representing on average 65% of the total $C_{37}$ alkenones, which is quite unusual for open ocean waters even cold and low salinity ones. However, $C_{37:4}$ have been reported in cold ocean surface waters of the North Atlantic and Nordic Seas (Sicre et al., 2002) yet at lower abundances (up to 35%). Percent of $C_{37:4}$ in estuarine sediments of Chesapeake Bay reached up to 40% of the total $C_{37}$ alkenones at temperature above 25°C (Mercer et al., 2005). This result indicates that besides marine producers local haptophyceae contributed to the production of this compound.

$U_{37}^{K'}$ values in Sermilik Fjord range from 0.31 to 0.47 (Fig. 4) contrasting with the lower values found in the coastal waters of Chesapeake Bay (0.118 to 0.313) (Mercer et al., 2005) and those found in a Norwegian fjord (Conte et al. (1994*)*. Higher $U_{37}^{K'}$ index in Sermilik fjord sediments therefore suggest a dominant marine alkenone source with only minor contribution of autochthonous haptophyceae in Sermilik fjord sediments. $U_{37}^{K'}$converted to SSTs using Prahl et al.'s calibration range between 8 and 12.5°C with a mean value of c. 10°C (Fig. 4). For comparison, SSTs calculated from the calibration establish by Mercer et al. (2005) ($U_{37}^{K'} = 0.013T-0.04$) for coastal/estuarine settings leads to unrealistic values ranging from 26.8 to 38.9°C, from which we hypothesize that the marine calibration likely provide better SST estimates and useful indication of its variability. SSTs along the core vary but are generally higher during the late 1930s and show a broad increase since 2000. Marked minima are observed in the 1960s, 1980s and 1990s.

# 5. Discussion

### *5.1 Sedimentation regime in the fjord*

A large number of sediment core studies from other East Greenland fjords; Kangerlussuaq (Syvitski et al., 1996; Smith & Andrews 2000), Nansen Fjord (Smith and Andrews 2000; Jennings and Weiner, 1996; Jennings et al., 2001) and Scoresbysund (Dowdeswell et al., 1993, 1994a; Ó Cofaigh & Dowdeswell 2001), also situated by marine-terminating glaciers, describe in details the characteristic sediment lithofacies and the glacial processes involved in their formation. This information has been used to study the sediment cores from Sermilik Fjord. The massive diamicton facies, with abundant pebbles in cores from the mid-part of the fjord, have been interpreted as resulting from iceberg delivery of heterogeneous debris under the assumption that sand grains are too large to be carried in suspension by the melt water plume. Calving variability of Helheim Glacier for the past 120 years has been reconstructed in a previous study (Andresen et al., 2012) by averaging three $^{210}Pb$ dated records, including ER07, of sand deposition (amount of sand deposited per year) taken from the mid-region of the fjord. The general conclusions from this study, thus taking into account changes in sand deposition in all three cores, are that iceberg discharge was markedly higher in the 1930s and 2000-2005 (Fig 5F).

The occurrence of microfossils (foraminifera and diatoms) is low in the mid-fjord cores, most likely because harsh environmental conditions in the fjord waters restrict biological productivity. Limited light penetration due to sea ice and icebergs and high loads of sediments in the turbid, fresh and cold surface waters will likely decrease the photosynthetic activity of phytoplankton inhabiting these fjord waters.

### *5.2 SST variability offshore Southeast Greenland*

The temperatures calculated from $C_{37:3}$ and $C_{37:2}$ relative abundances in ER07 sediments are found to be up to 8°C higher than the maximum summer temperatures observed in the upper 100 m of the fjord water column (<4°C, Fig. 2 and Straneo et al. 2010; 2011), suggesting that alkenones deposited in the fjord sediments are not primarily produced in the fjord. To account for this large offset, we hypothesize lateral advection of detrital alkenones from the Irminger warmer waters flowing from outside the fjord. This mechanism is consistent with the finding that Sermilik fjord waters are quickly and continuously replenished through a wind-driven exchange with the shelf (Straneo et al., 2010) thus allowing warm ‘detrital’ alkenones to enter the fjord and settle to the bottom floor. Several studies involving modern datasets already highlighted potential biases introduced by lateral advection of alkenones by strong surface ocean currents (Conte et al., 2006; Rühleman and Butzin, 2006; Mollenhauer et al., 2006). Sediments of the last glacial period from the Southern Indian Ocean revealed offsets between alkenone and foraminiferal transfer function SSTs due to advective transport of ‘warm’ alkenones by the Agulhas retroflection to the core site (Sicre et al., 2005). A similar phenomenon related to Irminger Sea Water transport by the East- and West Greenland Current system has been reported in the north eastern Labrador Sea during the last deglacial period by Knutz et al. (2011).

Our hypothesis is supported by a recent analysis of data from the Southeast Greenland shelf derived from deep diving seals tagged with satellite relay depths loggers equipped with temperature sensors (Sutherland et al., 2013). These data show that the water column in connection with the deep trough just outside Sermilik Fjord (Box 1 in Fig. 1B) is often characterized by 8-11°C warm water with no vertical variation during summer and fall (Fig. 2), and it was suggested that this warm water originates from the Irminger Current flowing along the continental slope. Indeed the temperature range derived from the seal data is similar to that recorded by alkenones deposited inside Sermilik Fjord. This supports the notion that the alkenones are mostly from outside the fjord and that they are indicative of water temperatures on the shelf region outside Sermilik Fjord and to a lesser degree also further upstream of the warmer waters of the IC. This conclusion is supported by Sutherland et al.’s (2013) observation that the region just outside Sermilik Fjord is a frontal region between warm surface IC and cold surface EGC. In such a region an associated enhanced vertical turbulent supply of nutrients (Gawarkiewicz, 1992) would sustain primary production, including prymnosiphytae, as also observed by more northerly frontal regions of the Denmark Strait (Thordardottir 1977; Knudsen and Eiríksson, 2002). Increased biological production in this area is also supported by the high concentration of seal dives recorded with respect to neighboring regions (Sutherland et al., 2013). Considering the temperature values of the upper waters inside the fjord (<4°C; Fig 2), local production is unlikely to have contributed significantly to sedimentary alkenone and it is therefore most probable that alkenone distributions reflect advection of subsurface waters into the fjord.

### *5.3 Assessing alkenone SSTs*

In order to evaluate the alkenone SSTs as reflecting SST variability outside Sermilik Fjord, they are compared with the Shelf Index established by Andresen et al. (2012) (Fig. 5D). Even though this data set is generated by data from regions relatively remote from Sermilik Fjord, they still belong to the same regional front system and should thus display the same temporal variability.

The Shelf Index was previously proposed (Andresen et al., 2012) to describe the oceanographic variability in Sermilik Fjord and the nearby shelf accounting for the combined variability of the presence of Irminger Water and Polar Waters. We briefly summarize it here. Variability in the IC was reconstructed using a time series from 1876 to 2007 of annual mean SSTs in an area south of Iceland, where the IC Waters upstream Greenland occupy a layer of several hundred meters extending to the surface (Fig. 5A). Periods of increased IC temperatures have been associated with a thickening of the Atlantic water layer (Våge et al., 2011). The Storis Index (Schmith and Hansen, 2005 and updated 2000-2007 in Andresen et al., 2012) is used as a proxy for Polar Waters. It is defined as the amount of multi-year sea ice that exits the Arctic Ocean via Fram Strait, around Cape Farewell and onto the SW Greenland shelf (Fig. 5B) and is available for the period 1820-2007. It has been defined as the northernmost position on the southwest coast, relative to Cape Farewell, of Storis exported through Fram Strait based on ice charts from the Danish Meteorological Institute (Valeur, 1976). A significant cross-correlation has been found between the Storis Index and the volume transport of sea-ice through Fram Strait derived from an ocean model (Schmith and Hansen, 2005). We use the Storis Index as a proxy for the Polar Water transport within the EGC assuming that the sea-ice export is correlated with the fresh water export through Fram Strait (Andresen et al., 2012). These Atlantic and Polar water records were subsequently normalised (by subtracting the mean and dividing by the standard deviation) and a Shelf Index was obtained by subtracting the resultant EGC Current index from the IC Water index. By doing so the two water masses are assumed weighted 1:1 in the Shelf Index in absence of information indicating different weighting of either water mass.  A positive (negative) Shelf Index implies increased (decreased) influence of Irminger Water and decreased (increased) influence from the EGC on the shelf.

The Shelf Index was previously assessed by comparison with repeat hydrographic surveys from Fylla Bank off Southwest Greenland (Andresen et al. 2012, Fig. 5C). The Fylla Bank surveys were performed for the 1950–2010 period (Ribergaard 2011) and extended back to 1876 (Ribergaard et al., 2008) using surface water temperature anomaly data (Smed, 1978). Even though these measurements are from the south-western side of Greenland, the continuity of the East and West Greenland Currents around Cape Farewell suggests that variability at Fylla Bank is also representative of the variability upstream by the southeast Greenland shelf and in the polar frontal zone (Bacon et al., 2008). The Shelf Index is statistically significant correlated with the Fylla Bank data (Andresen et al. 2012).

Similarities are observed between the alkenone-derived SST (Fig. 5E), the Shelf Index (Fig. 5D) and the Fylla Bank SSTs (Fig. 5C). Episodes with relatively warm conditions are recognised in the late 1930s and after 2000, as well as minor warming in the mid-1970s (red regions). During these warm periods, alkenone SSTs are slightly higher than those just outside the fjord emphasizing enhanced contribution of warmer IC waters which in summer can reach 11-12°C. The Great Salinity anomalies (GSAs), which occurred in the mid-1960/70s, 1980s and 1990s are all recognised as cooling episodes in both the alkenone SSTs, the Shelf index and the Fylla Bank data (blue stipled lines in Fig. 5). These were episodes with an increased amount of multi-year pack ice exported from the Arctic Ocean via the EGC. The episode in the mid-1960/70s was a more severe kind of a GSA, where the fresh surface water anomaly reached the northern coast of Iceland and was further transported with the WGC to the Labrador Sea and Newfoundland (Belkin, 2004).

We investigated the link between the alkenone-derived SSTs and the Shelf Index more statistically rigorously. Interannual variations are strongly damped in the proxy-based alkenone derived SST, and therefore we low-pass filtered the Shelf Index with a five year moving average so that the two series would get similar spectral characteristics. We then calculated their detrended correlation coefficient as 0.34. The two-sided 90% confidence band on this value was estimated by block-bootstrapping (Wilks, 1997) and we obtained the limits -0.04 and 0.56. Varying the block length between 5 and 15 years did not significantly change this.

The effect of uncertainties in the age model on the correlation coefficient was also considered. This was done by a Monte Carlo procedure where the age of each point in the record of alkenone SSTs was perturbed according to the uncertainties in the dating (fig 3c). From this we obtained a confidence band with limits 0.11 and 0.54. All this enable us to conclude with some justification that we have a relationship on the longer time scales between alkenone-derived SSTs and the Shelf Index.

Thus, comparison of the alkenone SSTs with the seal-derived SSTs and with the Shelf Index suggests that alkenones from Sermilik Fjord sediment reflect mainly SST changes outside Sermilik Fjord and to a lesser degree also further upstream of the warmer waters of the IC. Our results thus show that the observed alkenone SSTs variability is linked, to a certain degree, with shelf water property and variability caused by changes in the IC and EGC current systems.

### *5.4 Comparing reconstructed ocean temperature with glacier changes in Greenland*

The correspondence between climatic and oceanographic changes and the variability in the reconstructed changes in iceberg calving from Helheim Glacier was previously investigated (Andresen et al., 2012a). However, due to a lack of data from local hydrographical surveys, the calving record was compared with SST data from south of Iceland, the Storis Index and the Shelf Index assuming that the heat content of the waters reaching the glacier and its mélange may be linked to regional variability. It was found that on multi-decadal timescales, calving is linked with synchronous changes in the Northern Irminger Sea SSTs. SSTs in this region reflect the Atlantic Multi-decadal Oscillation (AMO), which is a multi-decadal mode of variability (oscillation of 65-70 years) occurring in the North Atlantic Ocean and is usually defined from patterns of SST variability; i.e. a positive (negative) mode is characterized by relatively high (low) SSTs (Schlesinger and Ramankutty, 1994). Furthermore, short-term (3-10 years) calving peaks were coincident with short-term episodes of positive Shelf Index indicating that increased IC inflow and/or warming along with decreased flow of Storis and EGC are associated with enhanced calving.

The alkenone SST data strengthens the link between oceanographic variability and Helheim Glacier calving (Andresen et al., 2012) with a detrended correlation coefficient of 0.37 and 90% confidence band with limits 0.09 and 0.56. Also the limits of the confidence band associated with uncertainties in the age model was estimated at 0.02 and 0.48 (see 5.3. for statistical method).

A new and interesting finding is that the alkenone SST data show a *record* peak in the late 1930s at the culmination of the so-called Early 20$^{th}$ Century Warming (Wood and Overland, 2010) and that it is broadly concordant with a calving maximum in 1940 (Fig. 5E and F). The upstream SSTs from south of Iceland do not show a *record* of high SST at this time – rather they resemble the AMO pattern with generally high SSTs in 1925-1965 (Fig. 5A). A possible explanation is that during the 1950s and 1960s the warm IC waters may have been mixed and cooled more intensively by the EGC upon reaching Southeast Greenland than during the 1930s and 1940s, when sea ice was less abundant and the EGC weaker (Schmith and Hansen, 2005, Fig. 5B). The same pattern of decreased ocean temperatures in the 1950-1960s is observed in West Greenland (Lloyd et al., 2011, Fig. 5G). In this study, benthic foraminifera assemblage changes in sediment cores obtained from Disko Bay by Jakobshavn Isbrae were used to reconstruct temperature variability at 300 m water depth. According to aerial images, a relatively rapid retreat of the Jakobshavn Isbrae glacier front occurred in 1930-1950, at the time of the subsurface water temperature maximum in 1920-1945 (peak in 1940). The glacier subsequently attained a stable position 1950-2000 and this stagnation was accompanied by a cold WGC in 1950-1980. Overall, these proxy-based ocean water temperature reconstructions document a markedly warm peak in subsurface water by West and surface water by Southeast Greenland in the late 1930s, possibly caused by less mixing of cold EGC waters at this time. Proxy-based temperature reconstructions of Greenland shelf waters detailing the past 100 years are restricted to the study presented here and the data set from Jakobshavn (Lloyd et al. 2011), but on the basis of these we suggest a period of markedly increased ocean heat content around 1940 impacted Greenland glacier stability to an extent that was only matched after 2000.

## 6. Conclusion

The alkenone SST record obtained from core ER07 provides evidence of repeated mixing of warm IC Water throughout the past 100 years into Sermilik Fjord. The temperature range of 8-12°C suggests that alkenones were produced outside the fjord and in the IC, and that production in the uppermost surface waters in the fjord was minor. The resemblance of alkenone SST variability with the Shelf Index emphasizes the regional character of this signal and its link to IC and EGC variability. Our results confirm previous finding on the important role of regional ocean forcing on outlet glacier stability, particularly the marked calving episode of the late 1930s. They also provide valuable information on the role of ocean and its heat content to Greenland Ice Sheet melting and succeeding sea level rise and emphasize the need to better account for ocean/sea ice interactions in modelling studies.

### Acknowledgements

This study has been supported by Geocenter Denmark in financial support to the SEDIMICE project, the Danish Council for Independent Research | Nature and Universe (Grant no. 09-064954/FNU) and the Danish Agency for Science, Technology and Innovation as part of the Greenland Climate Research Centre. The alkenone data presented here have been produced within the NAIV project supported by LEFE program of the Institut National des Sciences de l’Univers

(INSU) of the Centre national de la Recherche Scientifique. FS and DS were supported by NSF funded projects. We are very grateful to our reviewers for their help in improving this manuscript.

**References**

Andresen, C.S., Nørgaard-Pedersen, N., Jensen, J. B., Larsen, B., 2010. Southeast Greenland ice-sheet variability elucidated by shallow seismic survey and sediment coring in the Sermilik Fjord near the Helheim Glacier in 2009. Geological Survey of Denmark and Greenland Bulletin 20, 83-86.

Andresen, C. S., Straneo, F., Ribergaard, M. H., Bjørk, A. A., Andersen, T.J., Kuijpers, A., Nørgaard-Pedersen, N., Kjær, K. H., Schjøth, F., Weckström, K., Ahlstrøm, A. P., 2012. Rapid response of Helheim Glacier in Greenland to climate variability over the past century. Nature Geoscience 5, 37-41.

Appleby, P. G. and Oldfield, F. 1983. The assessment of $^{210}$Pb data from sites with varying sediment accumulation rates. Hydrobiologia 103, 29-35

Bacon, S., P.G. Myers, B. Rudels, and D.A. Sutherland (2008), Accessing the inaccessible: buoyancy-driven coastal currents on the shelves of Greenland and eastern Canada. *Arctic-Subarctic ocean fluxes: Defining the role of the Northern Seas in climate*. Eds. Dickson, Meincke, and Rhines.

Belkin, I.M., 2004. Propagation of the “Great Salinity Anomaly” of the 1990s around the northern North Atlantic. Geophysical Research Letters 31, L08306, doi:10.1029/2003GL019334.

Bendle, J., A. Rosell-Melé, and P. Ziveri,, 2005. Variability of unusual distributions of alkenones in the surface waters of the Nordic seas, Paleoceanography, 20, PA2001, doi:10.1029/2004PA001025.

Conkright, M. E., Locarnini, H. E., Garcia, T. D., O'Brien, T. P., Boyer, C. , Stephens, J., Antonov I., 2002. World Ocean Database 2001, vol. 1, Introduction, edited by S. Levitus, NOAA Atlas NESDIS 42, 167 pp., NOAA, Silver Spring, Md.

Conte, M. H., Thompson, A., Eglinton, G., 1994. Primary production of lipid biomarker compounds by *Emiliania huxleyi*: Results from an experimental mesocosm study in fjords of southern Norway. *Sarsia* 79, 319-331.

Conte, M. H., Sicre, M.-A., Rühlemann, C., Weber, J. C., Schulte, S., Schulz-Bull, D., Blanz, T. 2006. Global temperature calibration of the alkenone unsaturation index (UK'37) in surface waters and comparison with surface sediments, Geochem. Geophys. Geosyst., 7(2), Doi:10.1029/2005GC001054, 2006.

D'andrea, J.W., Y. Huang, S.C. Fritz and N.J. Anderson, 2011. Abrupt Holocene climate change as an important factor for human migration in West Greenland, PNAS, doi/10.1073/pnas.1101708108.

Dowdeswell, J.A., Whittington, R.J., Marienfeld, P., 1994. The origin of massive diamicton facies by iceberg rafting and scouring, Scoresby Sund, East Greenland. Sedimentology 41, 21-35.

Dowdeswell, J.A., Villinger, H., Whittington, R.J., Marienfeld, P., 1993. Iceberg scouring in Scoresby Sund and on the East Greenland continental shelf. Marine Geology 111, 37-53.

Dowdeswell, J.A., Whittington, R.J., Jennings, A.E., Andrews, J.T., Mackensen, A., Marienfeld, P., 2000. An origin for laminated glacimarine sediments through sea-ice build-up and suppressed iceberg rafting. Sedimentology 47, 557-576.

Enfield, D.B., Mestas-Nunez, A.M. and Trimble, P.J. 2001. The Atlantic Multidecadal Oscillation and its relationship to rainfall and river flows in the continental U.S.. *Geophys. Res. Lett.* 28, 2077-2080.

Gawarkiewicz, G., and D. C. Chapman (1992). The role of stratification in the formation and maintenance of shelf break fronts, J. Phys. Oceanogr., 22, 753– 772, doi:10.1175/1520-0485(1992)022<0753:TROSIT>2.0.CO;2.

Grimalt, J.O., Rullkötter J., Sicre M.-A., Harvey H.R., J.W. Farrington, Goni M., Sawada K. and Summons R., Modifications of the $C_{37}$ Alkenone and Alkenoate Composition in the Water Column and Sediment: Possible Implications for Sea Surface Temperature Estimates in Paleoceanography. *Geochemistry, Geophysics, Geosystems*, 2000GC000053, 2000.

Holland, D., Thomas, R., H., de Young, B., Ribergaard, M. H., Lyberth, B., 2008. Acceleration of Jakobshavn Isbrae triggered by warm subsurface ocean waters. Nature Geoscience 1, 659-664.

Howat, I. M., Joughin, I., Scambos, T.A., 2007. Rapid changes in ice discharge from Greenland Outlet Glaciers. Science 315, 1559-1561.

Howat, I. M., Smith, B. E., Joughin, I, Scambos T. A., 2008. Rates of southeast Greenland ice volume loss from combined ICESAT and ASTER observations. Geophys. Res. Lett., 35, L17505, doi:10.1029/2008GL034496.

Jennings, A.E., Weiner, N.J., 1996. Environmental changes in eastern Greenland during the last 1300 years: evidence from foraminifera and lithofacies changes in Nansen Fjord, 68ºN. The Holocene 6 (2), 179–191.

Jennings, A. E. Knudsen, K. L., Hald, M, Hansen, C. V., Andrews, J. T., 2001. A mid-Holocene shift in Arctic sea-ice variability on the East Greenland Shelf The Holocene 2002; 12; 49, DOI: 10.1191/0959683602hl519rp

Knudsen, K.L., Eiríksson J., 2002. Application of tephrochronology to the timing and correlation of palaeoceanographic events recorded in Holocene and Late Glacial shelf sediments off North Iceland. Marine Geology 191, 165-188.

Knutz, P. C., Sicre, M.-A., Ebbesen, H., Christiansen, S., Kuijpers A., 2011. Multiple-stage deglacial retreat of the southern Greenland Ice Sheet linked with Irminger Current warm water transport, Paleoceanography 26, PA3204, doi:10.1029/2010PA002053.

Luckman, A., Murray, T., de Lange, R., Hanna, E., 2006. Rapid and synchronous ice-dynamic changes in East Greenland, Geophys. Res. Lett. 33, L03503, doi:10.1029/2005GL025428.

Lloyd, J.M., Moros, M., Perner, K., Telford, R., Kuijpers, A., Jansen, E., McCarthy, D, 2011. A 100 year record of ocean temperature control on the stability of Jakobshavn Isbrae, West Greenland. Geology 39, 867-870.

Malmberg, S.-A. 1985. The water masses between Iceland and Greenland. J. Mar. Res. Inst. 9, 12-140

Mercer, J.L., Zhao, M., Colman, S.M., 2005. Seasonan variations of alkenoens and $U^{K'}_{37}$ in the Chesapeake Bay water column. Estuarine, and Coastal and Shelf Sciences, 63, 675-682.

Mernild, S. H., Howat, I. M., Ahn, Y., Liston, G. E., Steffen, K., Jakobsen, B. H., Hasholt, B., Fog, B., van As, D., 2010. Freshwater flux to Sermilik Fjord, SE Greenland. The Cryosphere, 4, 453–465. www.the-cryosphere.net/4/453/2010/ doi:10.5194/tc-4-453-2010

Moon, T., Joughin I., 2008. Changes in ice front position on Greenland's outlet glaciers from 1992 to 2007. Journal of Geophysical Research-Earth Surface 113(F2), 10.

Mollenhauer, G., McManus, J.F., Benthien, A., Muller, P.J., Eglinton, T.I. 2006. Rapid lateral particle transport in the Argentine Basin: molecular 14C and 230 Thxs evidence. Deep-Sea Research I 53, 1224-1243.

Murray, T., Scharrer, K., James, T.D., Dye, S.R., Hanna, E., Booth, A.D., Selmes, N., Luckman, A., Hughes, A.L.C., Cook, S., Hybrechts, P., 2010. Ocean regulation hypothesis for glacier dynamics in southeast Greenland and implications ice sheet mass change. J Geophys Res 115(F03026). doi:10.1029/2009JF001522.

Nick, F. M., Vieli, A., Howat I.M., Joughin, I., 2009. Large-scale changes in Greenland outlet glacier dynamics triggered at the terminus. Nature Geoscience doi:10.1038/ngeo394

Ó Cofaigh, C., Dowdeswell, J.A., Grobe, H., 2001. Holocene glacimarine sedimentation, inner Scoresby Sund, East Greenland: the influence of fast-flowing ice sheet outlet glaciers. Marine Geology 175, 103-129.

Prahl, F. G., Muehlhausen, L. A., Zahnle, D. L., 1988. Further evaluation of long-chain alkenones as indicators of Paleoceanographic conditions, Geochemica Cosmochimica Acta, 52, 2303–2310.

Prahl, F., Herbert, T., Brassell, S. C., Ohkouchi, N., Pagani, M., Repeta, D., Rosell-Melé, A. and Sikes, E. 2000. Status of alkenone paleothermometer calibration: Report from Working Group 3. Geochem, Geophys. Geosys 1, 2000GC000058

Ribergaard, M.H., 2011. Oceanographic Investigations off West Greenland 2010. NAFO Scientific Council Documents 11/001.

Ribergaard, M.H., Olsen, S.M., and Mortensen, J., 2008. Oceanographic Investigations off West Greenland 2007. NAFO Scientific Council Documents 08/003.

Rignot, E., and S. S. Jacobs, 2002. Rapid bottom melting widespread near Antarctic ice sheet grounding lines. Science 296, 2020–2023.

Rignot, E., Kanagaratnam, P., 2006. Changes in the velocity structure of the Greenland Ice Sheet. Science 311(5763), 986–990.

Rignot E., Koppes, M., Velicogna I., 2010. Rapid submarine melting of the calving faces of West Greenland glaciers. Nature Geoscience 3, 187–191.

Rühlemann, C., Butzin, M., 2006. Alkenone temperature anomalies in the Brazil-Malvinas Confluence area caused by lateral advection of suspended particulate material, Geochemistry Geophysics Geosystems, 7, Q10015, doi:10.1029/2006GC001251

Schlesinger, M. E., Ramankutty, N., 1994. An oscillation in the global climate system of period 65–70 years. Nature 367, 723–726.

Schjøth, F., Andresen, C.S., 2010. From unknown sea bed morphology in the Sermilik Fjord, Southeast Greenland to a bathymetric map based on more than 500.000 echo sounder and Chirp sub-bottom profiler measurements (abstract & poster). ESRI Europe, Middle East and Africa User Conference. 26 – 28 october, 2010, ESRI Italia, Rome, Italy.

Schmith, T., Hansen, C., 2005. Fram Strait Ice Export during the Nineteenth and Twentieth Centuries Reconstructed from a Multiyear Sea Ice Index from Southwestern Greenland. Journal of Climate 16, 2782−2791 (2003).

Schulz, H.-M., A. Schöener, and K.C. Emeis, 2000. Long-chain alkenone patterns in the Baltic Sea—an ocean-freshwater transition, Geochimica et Cosmochimica Acta, 64, 469–477.

Sicre, M.-A., Jacob, J., Ezat, U., Rousse, S., Kissel, C., Yiou, P., Eiríksson, J., Knudsen, K.L., Jansen, E., Turon, J.-L., 2008. Decadal variability of sea surface temperatures off North Iceland over the last 2000 years. Earth and Planetary Science Letters 268: 137-142.

Sicre M.-A., E. Bard, U. Ezat and F. Rostek, Alkenone distributions in the North Atlantic and Nordic sea surface waters, Geochemistry, Geophysics, Geosystems, doi: 2001GC000159, 2002.

Sikes, E.L. and Sicre M.-A., The relationship of the tetra-unsaturated $C_{37}$ alkenone to salinity and temperature: implication for paleo-studies, Geochemistry, Geophysics, Geosystems, doi: 2002GC000345, 2002.

Sicre, M.-A., Labeyrie L., Ezat, U. Duprat, J. Turon J-L, Schmidt S., Michel E. and Mazaud A., Southern Indian Ocean response to Northern Hemisphere Heinrich events. Earth and Planetary Science Letters **240**, 724-731, doi: 10.1016, 2005.

Smed, J., 1978. Fluctuations in the temperature of the surface water in the areas of the northern North Atlantic, 1876–1975. In: Danish Meteorological Institute Climatological Papers, **4**. p 205–210.

Smith, L. M., Clark, A., Jennings, A. E. 2002. Accumulation in East Greenland Fjords and on the continental shelves adjacent to the Denmark Strait over the last century based on $^{210}Pb$ geochronology. Arctic 55, 109-122.

Stearns, L. A., Hamilton, G. S., 2007. Rapid volume loss from two East Greenland outlet glaciers quantified using repeat stereo satellite imagery. Geophys. Res. Lett. 34, L05503, doi:10.1029/2006GL028982 (2007).

Straneo, F., Hamilton, G. S., Sutherland, D. A., Stearns, L. A., Davidson, F., Hammill, M. O., Stenson, G. B., Rosing-Asvid, 2010. Rapid circulation of warm subtropical waters in a major glacial fjord in East Greenland. Nature Geoscience 3, 182-186.

Straneo, F., R. Curry, D.A. Sutherland, G. Hamilton, C. Cenedese, K. Väge, L.A. Stearns, 2011: Impact of fjord dynamics and subglacial discharge on the circulation near Helheim Glacier in Greenland. Nature Geoscience, doi:10.1038/ngeo1109.

Straneo, F., D. A. Sutherland, D. Holland, C. Gladish, G. Hamilton, H. Johnson, E. Rignot, Y. Xu, M. Koppes, 2012: Characteristics of ocean waters reaching Greenland's glaciers. Annals of Glaciology, 53(60), 202-210.

Sutherland, D.A., Pickart, R. S., 2008. The East Greenland Coastal Current: structure, variability, and forcing. Progress in Oceanography, doi:10.1016/j.pocean.2007.09.006.

Sutherland, D., F. Straneo, G.B. Stenson, F. J.M. Davidson, M. O. Hammill, A. Rosing-Asvid, 2013: Atlantic water variability on the SE Greenland continental shelf and its relationship to SST, J. Geophys. Res. Oceans, 118-1-9, doi:10.1029/2012JC008354

Syvitski, J. P. M., Andrews, J. T., Dowdeswell, J. A. 1996. Sediment deposition in an iceberg-dominated Glacimarine Environment, East Greenland: Basin Fill Implications. Global and Planetary Change 12, 251-270.

Ternois Y., Sicre M. -A., Boireau A., Conte M. H., Eglinton, G. 1997. Evaluation of long-chain alkenones as paleo-temperature indicators in the Mediterranean Sea. Deep-Sea Res. 44, 271–286.

Ternois Y., Sicre M.-A., Boireau A., L. Beaufort, J-C Miquel and C. Jeandel, Hydrocarbons, sterols and alkenones in sinking particles in the Indian sector of the Southern Ocean. *Organic Geochemistry 28*, 489-501, 1998.

Thordardóttir T., 1977. Primary production in North Icelandic waters in relation to recent climatic change. In Polar Oceans: Proceedings of the polar oceans conference held at McGill University, Montreal, in May 1974, pp. 655–665. Ed. By M. J. Dunbar. SCOR/SCAR, Canada. 681 pp.

Valeur, H.H.. Polar ice variations off the Greenland west coast 1900–72. *Int. Commission for the Northwest Atlantic Fisheries*, Special Publication **9**, 27 pp. (1976).

Van den Broeke, M.R., Bamber, J., Ettema, J., Rignot E., Schrama, E., van de Berg, W. J., van Meijgaard, E., Velicogna, I., Wouters, B., 2009. Partitioning recent Greenland mass loss. Science 326, 984-986.

Vieli, A., and F. M. Nick (2011), Understanding and modeling rapid dynamic changes of tidewater outlet glaciers: issues and implications. Surv.
Geophys., 32, doi:10.1007/s10712-011-9132-4.

Volkman, J. K. 2000. Ecological and environmental factors affecting alkenone distributions in seawater and sediments, Geochem. Geophys. Geosyst. 1, 2000GC000061.

Våge, K., Pickart, R. S., Sarafanov, A., Knutsen, Ø., Mercier, H., Lherminier, P., van Aken, H. M., Meincke, J., Quadfasel, D., Bacon, S., 2011. The Irminger Gyre: Circulation, convection, and interannual variability. Deep Sea Research Part I: Oceanographic Research Papers 58(5), 590–614.

Wilks, D. S., 1997: Resampling hypothesis tests for autocorrelated fields. J. Climate, 10, 65–82.

Wood, K. R., Overland, J. E., 2010. Early 20th century Arctic warming in retrospect. Int. J. Climatol. 30: 1269–1279. DOI: 10.1002/joc.1973.

**Figure captions**

Fig 1. A. Main currents in the North Atlantic Ocean (Straneo et al., 2012) and location of Helheim Glacier (HG), Kangerdluqssuaq Glacier (KG), Disko Bay (DB), Jakobshavn Isbrae (JI), Scoresbysund (SU), Fyllas Banke (FB) and region south of Iceland from where SSTs of the IC were obtained. B. Helheim Glacier and Sermilik Fjord with position of core ER07 (bathymetry from Schjøth et al., 2012) and the pathways of the EGC/EGCC system and the IC (Straneo et al., 2010). Box 1 indicates the region in which the alkenone-derived SST reconstruction is interpreted to record variability.

Fig. 2. Profiles of temperature versus depth taken inside Sermilik Fjord during the summers of 2008, 2009, 2010 and 2011 (blue) via ship-based hydrography (the 2008 and 2009 are those described in Straneo et al. 2010; 2011) and outside the fjord via tagged seals (red, see Box 1 in Fig. 1B). The seal-derived temperatures represent summer/fall conditions when Irminger Sea water was present (29% of all profiles) over the time period 2004—2010 (Sutherland et al. 2013).

Fig. 3. Core ER07 sedimentology and chronology (Andresen et al., 2012). A. Grain size distribution (wt%) of clay, silt and sand. B. Unsupported $^{210}$Pb and $^{137}$Cs. C. Age model based on $^{210}$Pb and $^{137}$Cs dating (one sigma error bars).

Fig. 4. Core ER07 U37k' values (left axis) and alkenone-derived SST data (right axis). Internal precision is estimated to 0.5°C.

Fig. 5. Comparison with other records. A. SST from offshore South Iceland (black line 3 point running mean). The AMO Index (from Enfield et al. 2001) is shown above (3 point running annual mean). Red (blue) scrapings indicate positive (negative) Index. B. The Storis Index (black line 3 point running mean). C. The shelf Index (black line 3 point running mean). D. Fylla Banke SST (black line 3 point running mean) (Ribergaard et al., 2011). E. ER07 alkenone-derived SST (black line 3 point running mean). F. Reconstructed calving variability of Helheim Glacier. Data in A-C and F from Andresen et al., 2012. G. % Warm water foraminifera in Egedesminde Dyb by Disko Bay (Lloyd et al., 2012). Warm SST episodes in alkenone data highlighted with red boxes. Blue stipled lines indicate Great Salinity Anomalies (GSAs).

Figure
Click here to download high resolution image

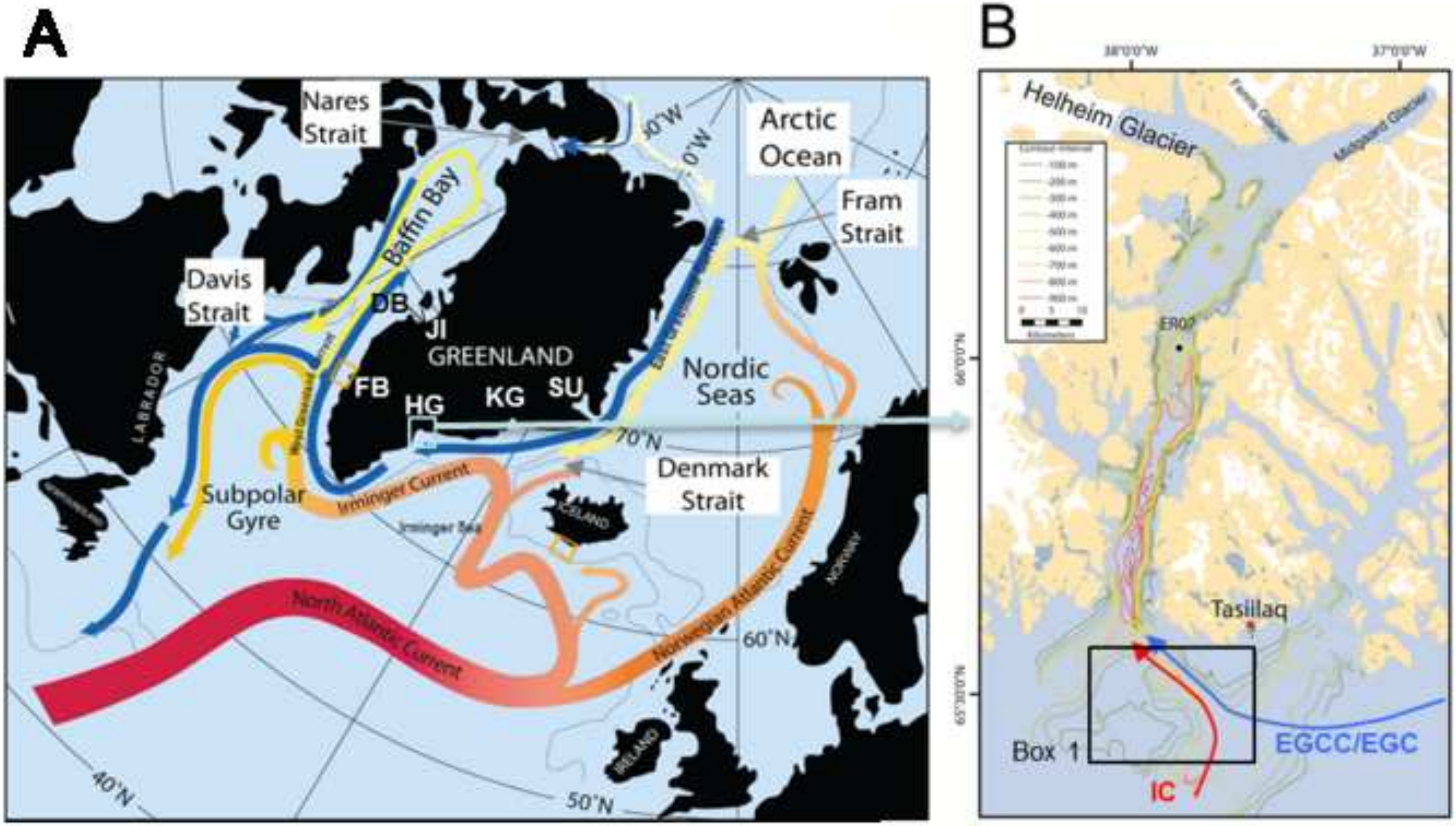

**Figure**
**Click here to download high resolution image**

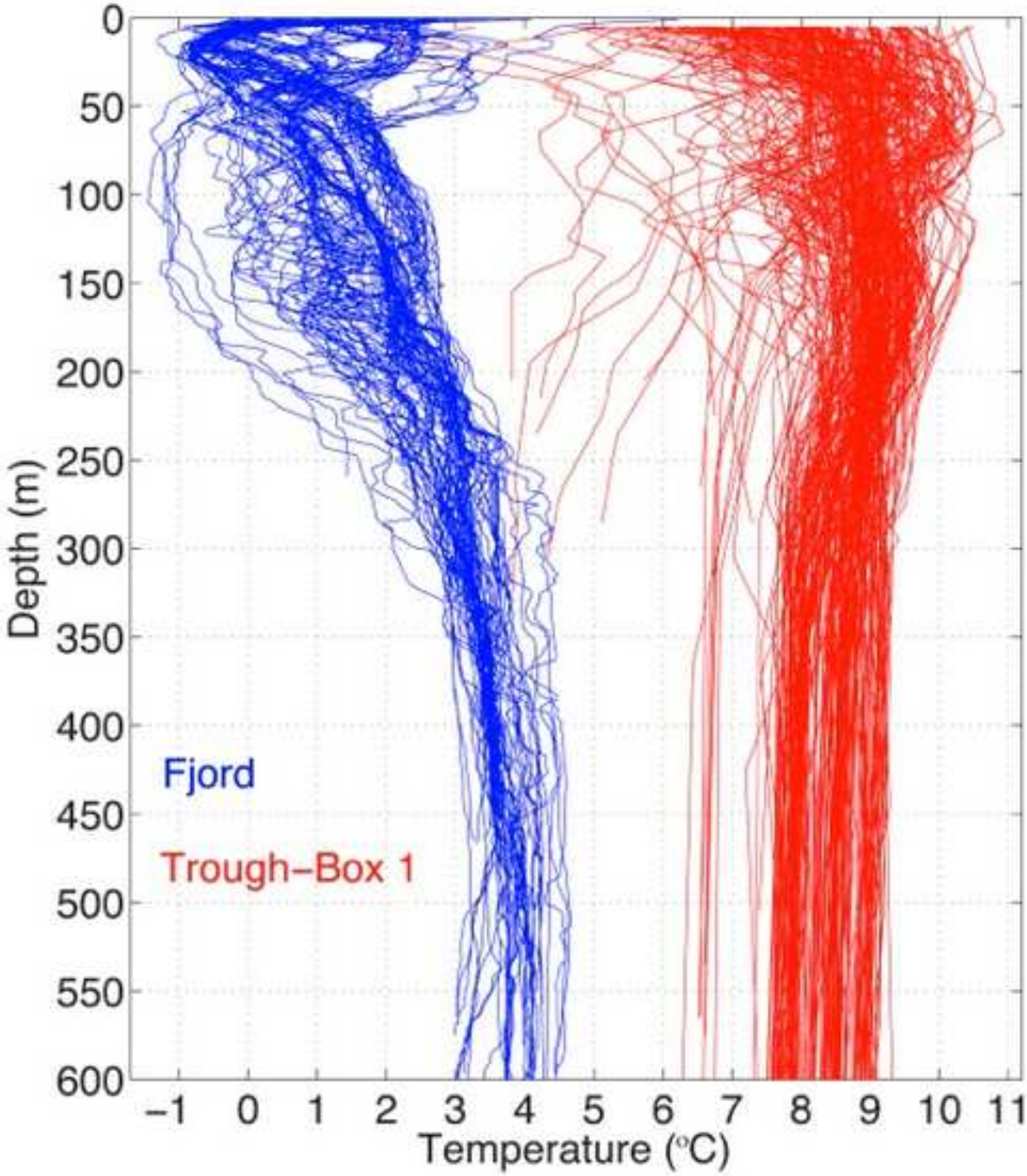

Figure
Click here to download high resolution image

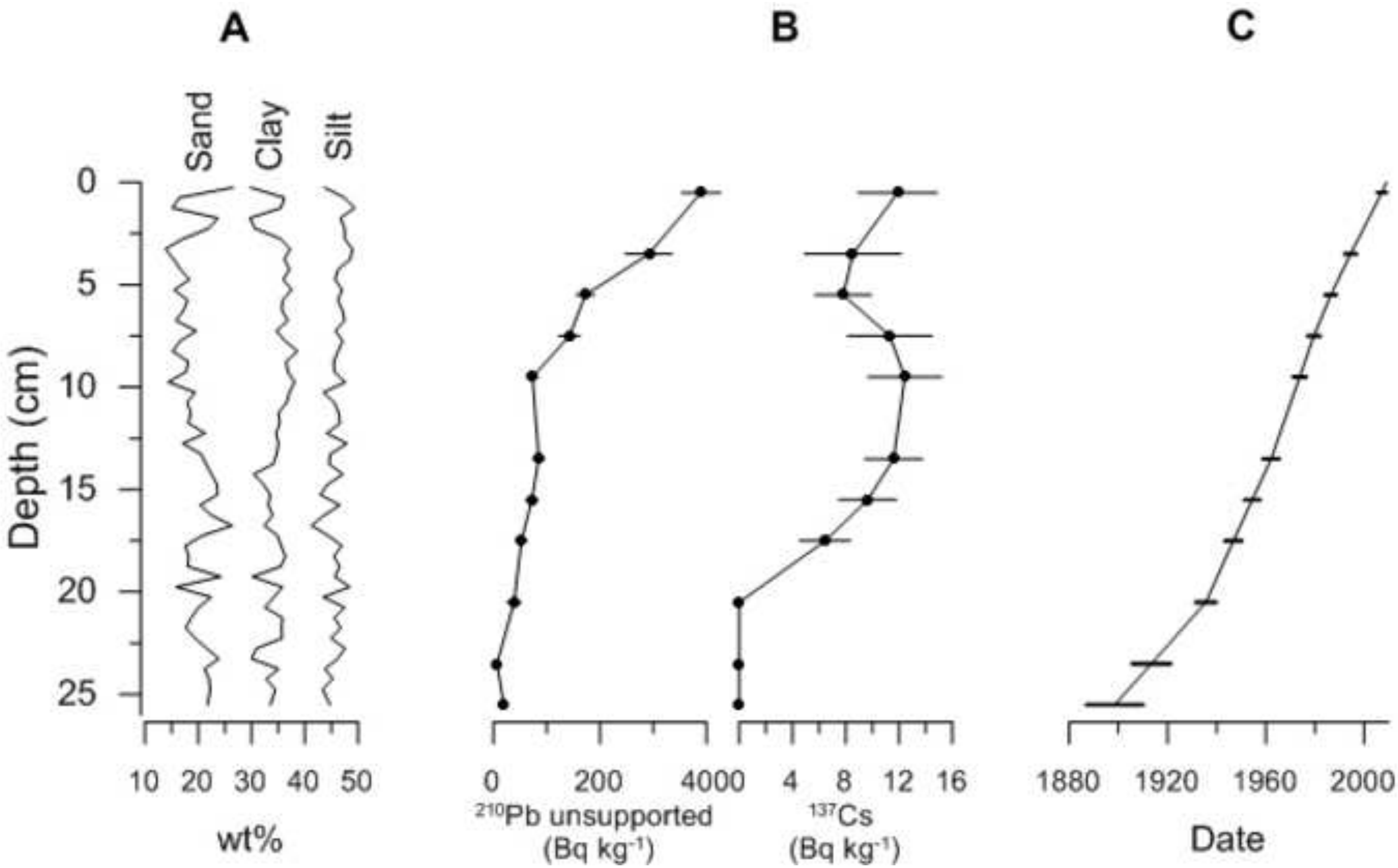

Figure
Click here to download high resolution image

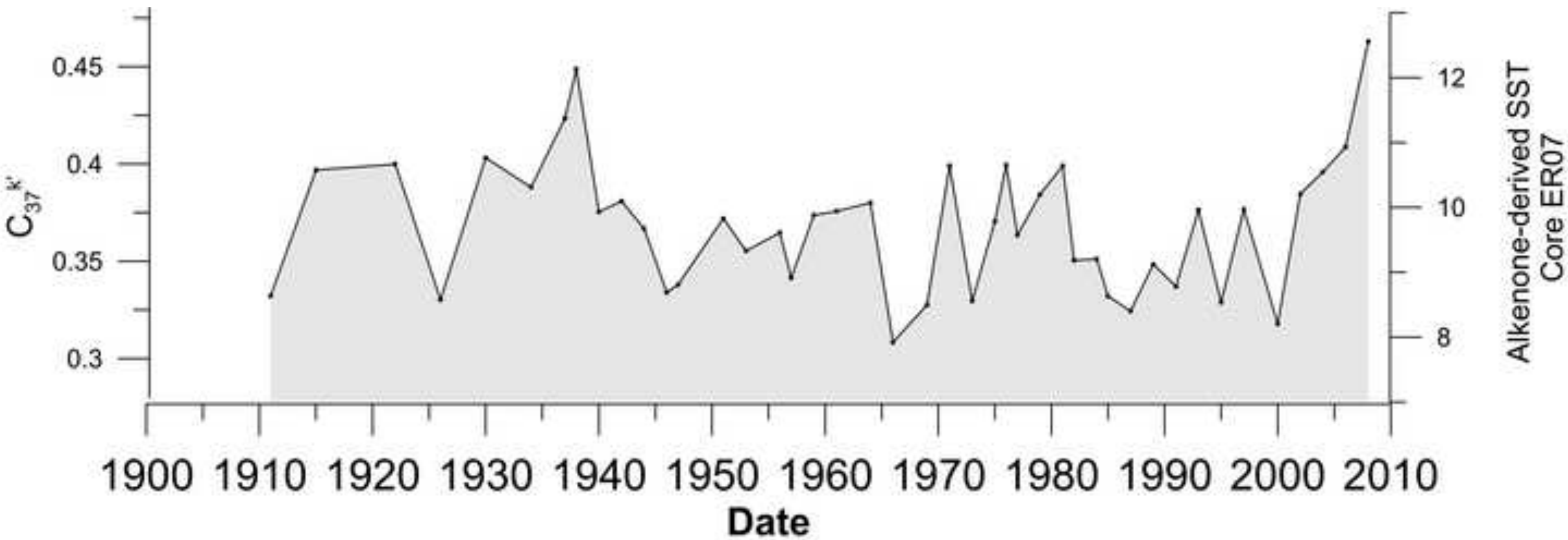

**Figure**

**Click here to download high resolution image**